tvst

https://doi.org/10.1167/tvst.7.6.7

Article

Noninvasive Assessment of Retinal Blood Flow Using a Novel Handheld Laser Speckle Contrast Imager

Abhishek Rege[1], Samantha I. Cunningham[1], Yusi Liu[1], Karan Raje[1], Sachin Kalarn[2], M. Jason Brooke[1], Lisa Schocket[2], Sunni Scott[2], Asifa Shafi[2], Luis Toledo[2], and Osamah J. Saeedi[2]

[1] Vasoptic Medical Inc., Baltimore, MD, USA
[2] Department of Ophthalmology and Visual Sciences, University of Maryland Baltimore, Baltimore, MD, USA

Correspondence: Osamah J. Saeedi, 419 W Redwood St, Suite 470, Baltimore, MD 21201, USA. e-mail: osaeedi@som.umaryland.edu

Received: 3 February 2018
Accepted: 8 September 2018
Published: 14 November 2018

Keywords: laser speckle imaging; retinal blood flow; ocular imaging

Citation: Rege A, Cunningham SI, Liu Y, Raje K, Kalarn S, Brooke MJ, Schocket L, Scott S, Shafi A, Toledo L, Saeedi OJ. Noninvasive assessment of retinal blood flow using a novel handheld laser speckle contrast imager. Trans Vis Sci Tech. 2018;7(6):7, https://doi.org/10.1167/tvst.7.6.7

Copyright 2018 The Authors

Purpose: We assessed the image quality and reproducibility of blood flow measurements from a novel handheld laser speckle imager in handheld and stabilized use cases.

Methods: Eleven dilated human subjects were imaged with the XyCAM Handheld Retinal Imager investigational device (XyCAM HRI) in the handheld and stabilized use case in nine consecutive imaging sessions. Subjects then underwent standard color fundus photography using a Topcon TRC 50DX. The vessel-to-background contrast of the XyCAM HRI red-free photo was compared to the fundus photograph, while the coefficient of variation of blood flow measurements in specific arteries and veins also was determined.

Results: Vessel-to-background contrast was statistically greater in the handheld use case when compared to the standard color fundus photographs ($P = 0.01$). Estimates of mean blood flow velocity (BFV) were highly correlated between the stabilized and handheld use case ($r^2 = 0.96$). Peak velocity estimates in arteries were significantly higher than those in veins ($P < 0.05$).

Conclusions: The XyCAM HRI prototype can acquire fundus photographs with the same or better level of clarity as color fundus photographs, and reproducibly acquire functional blood flow information in the handheld use case.

Translational Relevance: To our knowledge, this is the first human study of a handheld laser speckle retinal imaging device. Determination of retinal blood flow has applications to ophthalmic and systemic disease and a portable handheld retinal imager that determines blood flow may be widely adopted at the point of care.

Introduction

Assessment of retinal blood flow (RBF) has a potential role in the diagnosis of ophthalmic conditions, such as diabetic retinopathy,[1–3] hypertensive retinopathy,[4] and glaucoma,[5,6] as well as systemic conditions, including stroke,[7–10] hypertension-related cardiovascular complications,[11,12] and Alzheimer's disease.[13] Clinical diagnostics and decision support for these diseases may be facilitated through a nuanced assessment of retinal vasculature, which includes measurement of retinal vessel caliber, tortuosity, density, and RBF. While it is possible to estimate caliber and tortuosity from fundus photographs, estimation of RBF requires sophisticated instrumentation that currently is not available to primary care providers due to cost and size/space limitations.

Numerous devices and techniques have been developed to measure retinal blood flow, starting from the measurement of transit time of fluorescein,[14] to more advanced noninvasive techniques, such as laser Doppler flowmetry,[15] laser speckle angiography,[16] and recently optical coherence tomography angiography (OCTA).[17] Generally, these techniques require costly and large devices. While there are currently no United States Food and Drug Admin-

This work is licensed under a Creative Commons Attribution-NonCommercial-NoDerivatives 4.0 International License.

istration (FDA)–approved handheld retinal blood flow devices, a stationary mounted portable imager has been used to monitor ocular blood flow during cardiac surgery.[18]

The XyCAM Handheld Retinal Imager (XyCAM HRI) investigational device (Vasoptic, Inc., Baltimore, MD) is a low-cost, handheld, portable, retinal blood flow imaging system designed for use at the point of care. This device uses Laser Speckle Contrast Imaging (LSCI) to determine retinal blood flow and also captures a red-free fundus photo simultaneously. LSCI is a noninvasive technique that uses a low intensity laser to cause speckle formation, which then is analyzed to quantify the amount of blurring that is caused by the motion of red blood cells within vessels. Speckle images of the retina can be processed to quantify the extent of blurring resulting in estimates of vessel-specific blood flow information with high spatiotemporal resolution. The XyCAM HRI prototype uses a combination of fundus photography and LSCI to capture vessel diameters and degree of vessel proliferation, as well as discriminate arterial from venous physiology.

We described the results of an early feasibility clinical study of the XyCAM HRI prototype. We assessed the image quality of the red-free fundus photo as well as the reproducibility of XyCAM-based flow measurements in the handheld and bench-mounted stabilized use cases. We hypothesize that the XyCAM prototype can produce high quality retinal images and reproducible blood flow measurements, and that RBF measurements taken from the handheld XyCAM prototype are comparable with the bench-mounted XyCAM prototype.

Methods

Participants

All clinical experimentation was performed at the Department of Ophthalmology and Visual Sciences of the University of Maryland Baltimore (UMB), with approvals from the University of Maryland Baltimore institutional review board. Individuals were recruited from either the optometry clinic or retina subspecialty clinic at UMB and received monetary compensation for their participation. Informed consent was obtained from the subjects after explanation of the nature and possible consequences of the study. This research followed the tenets of the Declaration of Helsinki.

The inclusion and exclusion criteria used to enroll subjects are listed in Table 1. Eleven individuals (four males; mean age ± standard deviation [SD], 55.6 ± 11.7 years; range, 23–75 years; Table 2) participated in the study. Six additional individuals also were enrolled in the study, but were excluded from analysis for the following reasons: two subjects failed to complete all study procedures (one subject's session was aborted due to their incidental high blood pressure before imaging, and a second subject's session was terminated following an interruption because of technical difficulties), three subjects presented with pupils that dilated to <4 mm, which was suboptimal to the intended use case, and data acquired from a sixth subject did not include the retinal regions of interest evaluated in this study. Healthy subjects included diabetic ($n = 5$), prediabetic ($n = 2$), and nondiabetic ($n = 4$) individuals, as determined during subject screening procedures. However, no subject was diagnosed with diabetic

Table 1. Inclusion and Exclusion Criteria for Enrollment of Healthy Participants Into the Imaging Study

Inclusion criteria	• Presented to ophthalmology/optometry clinic for eye examination • Capable of giving informed consent and complying with the restrictions and requirements of the protocol • ≥18 years old with binocular vision
Exclusion criteria	• Significant media opacity (e.g., a visually significant cataract or significant corneal scar) • Prior ocular surgery other than uncomplicated cataract extraction • Prior ocular disease (including patients that are glaucoma suspects) other than moderate to severe nonproliferative diabetic retinopathy • Anatomically narrow angles or a prior adverse reaction to administration of tropicamide • Significant vascular risk • Significant abnormalities on dilated fundus exam • >4 diopters of refractive error • Female who is pregnant or of childbearing age • Implantable device (e.g., a pacemaker or an implantable cardioverter defibrillator)

Table 2. Subjects Demographic and Vision Information

	Subject ID	Age, Years	Sex	Diabetes Status	Imaged Eye
Training data	S1	59	F	DM	R
	S2	59	M	None	R
	S3	58	F	Pre-DM	R
	S4	58	M	None	R
	S5	61	F	None	R
Statistical	S6	23	M	None	R
assessment	S7	75	F	DM	R
(test) data	S8	55	F	Pre-DM	R
	S9	55	F	DM	R
	S10	54	M	DM	R
	S11	55	F	DM	R

DM, Diabetes Mellitus; R, Right; M, Male; F, Female.

retinopathy, which could have influenced the vascular characteristics of the retina.

System Description

The XyCAM HRI prototype is a portable retinal blood flow monitor weighing 0.9 kg with a resolution of 48 linear pixels per degree of retinal field of view. It can be used either in a handheld manner in conjunction with a handle, or mounted on a slit-lamp base for stabilized use as in traditional ophthalmic photography settings (Figs. 1A, 1B). In both cases, the device contains a dual illumination module that emits green (peak 523 nm) noncoherent light for high contrast fundus photography and a low-power red (650 nm) laser for LSCI. During an imaging session, image acquisition is synchronized with the illumination: a remote controller is used to trigger the sequential acquisition of up to 10 fundus image frames in green light illumination and up to 160 speckle image frames under red laser illumination. Images then are acquired using a sensitive 16-bit monochrome CMOS camera at a frame rate of >60 frames per second. Illumination intensity, optical focusing, and image acquisition functions may be adjusted further using the remote controller and custom software developed in MATLAB (MathWorks, Natick, MA). An on-device screen displays a live view of the imaging target.

Clinical Procedures

Before clinical investigation, the XyCAM HRI prototype was tested for conformance with safety guidelines established by the International Organization of Standardization (ISO)[19] and International Electrotechnical Commission (IEC).[20] The measured power of the laser at the beam waist was 65 microwatts, making it a Class I laser and a Group 1 ophthalmic instrument. The study was further deemed a nonsignificant risk study by the FDA.

All subjects completed a single imaging visit, which first included collection of patient blood pressure (BP), heart rate, height, and weight measurements using standard clinical instruments. Subsequently, subjects underwent a series of two trials with the XyCAM prototype to assess use of the device in: (1) a stabilized use case in which the device was mounted on a stand while the individual's head was stabilized on a standard clinical chin rest during imaging, and (2) a handheld use case in which the operator held the device while stabilizing their hand gently on the subject's cheek. Each trial consisted of four imaging sessions to acquire morphologic and physiologic images of a region of interest (ROI) centered on the optic nerve head (ONH) in the right eye. One attending physician (OS) and one physician-in-training (SK) completed imaging for all patients, but only one operator at a time was required to acquire these data.

Testing was performed following pupil dilation of the imaged eye. Pupillary dilation was achieved via administration of 1% tropicamide. Upon confirmation that the pupil had dilated to ≥5 mm in diameter, Trial 1 was conducted under stabilized use case settings. The XyCAM prototype was affixed to a precision stand and positioned in front of the subject's eye (Fig. 1A) while the subject rested their head on a chin-rest accessory. Using a live view of the target under green light illumination, the operator then repositioned the device as necessary using controls on the precision stand to ensure the desired ONH ROI was within the FOV. Positioning of the ONH in the FOV was further accomplished by having subjects fixate on a standalone external target or low intensity LED fixation attached to the device that could be manipulated by the operator. After positioning and focusing of the ONH in the FOV was deemed satisfactory, a second operator initiated image acquisition by triggering the device's remote controller capture button. Upon manual triggering, five fundus photographs under green illumination and 120 speckle images under red laser illumination were sequentially and automatically acquired. Raw image data were stored for offline processing. This procedure was repeated three additional times (with a delay

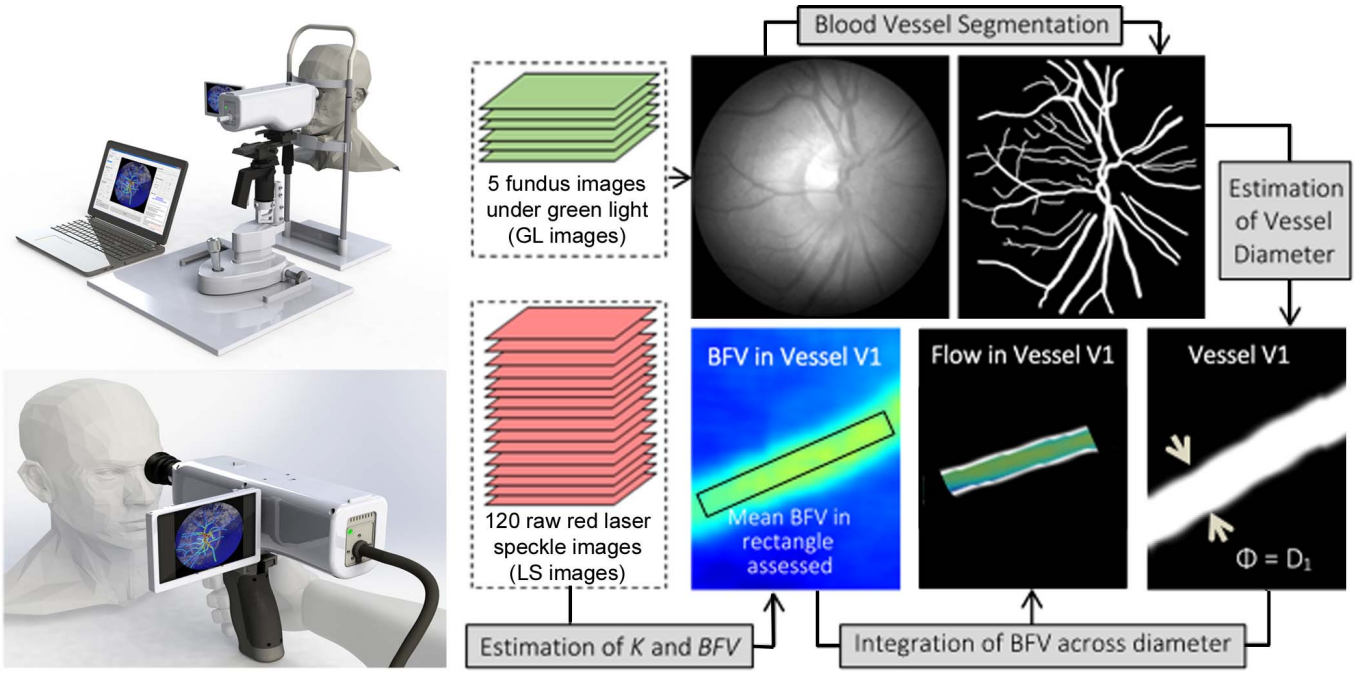

Figure 1. Illustration of the experimental setup for data acquisition using the XyCAM HRI and analysis of acquired data. (A) Stabilized setup. (B) Handheld setup. (C) Image acquisition and processing methodology, including creation of blood flow maps, manual creation of vessel ROIs, and generation of ROI-specific blood flow maps. N, number of speckle image frames acquired; M, number of frames used for spatiotemporal contrast calculation of one LSCI image; RVBF, retinal vessel blood flow images in vessels of interest.

of 1 to 2 minutes between each imaging session) for a total of four imaging sessions.

Following Trial 1, the XyCAM HRI prototype was removed from the precision stand and a handle accessory was attached to the base of the device for handheld use by the operator. Device stabilization during handheld imaging was achieved by resting the device against the operator's free hand, which itself was rested against the subject's cheek. The same positioning and image acquisition procedures described for Trial 1 then were completed for Trial 2, including acquisition of four image datasets.

Following image acquisition with the XyCAM HRI prototype, subjects completed a third trial consisting of one imaging session using a Topcon TRC 50DX (Topcon, Tokyo, Japan) fundus photography device. A minimum of four color fundus images containing the ONH region were obtained using standard clinical practice and used as reference images.

Image Processing and Analysis

Speckle images were processed in MATLAB by first extracting a measure called speckle contrast (K) — the ratio of standard deviation of pixel intensities to the mean pixel intensity within a spatio-temporal neighborhood around every pixel P_0 (Equation 1):

$$K(P_0) = \sigma_{\mathbb{N}(P_0)} / \mu_{\mathbb{N}(P_0)} \quad (1)$$

where $\sigma_{\mathbb{N}(P_0)}$ and $\mu_{\mathbb{N}(P_0)}$ are the standard deviation and mean, respectively, in the intensity of all pixels on a defined local neighborhood $\mathbb{N}(P_0)$. Speckle contrast may be calculated such that $\mathbb{N}(P_0)$ is chosen in either the spatial domain called sLSCI[21] or the temporal domain called tLSCI.[22] Exclusively spatial processing preserves temporal resolution by requiring that only $N = 1$ image frame is acquired, while temporal processing requires the acquisition of $N = 80$ image frames to provide higher spatial resolution with a compromised temporal resolution. To optimize image acquisition times and resolution in spatial and temporal domains, K was calculated from the XyCAM HRI prototype speckle images using a spatiotemporal pixel-neighborhood of 5 pixels × 5 pixels (spatial window, S) × 5 frames (temporal window, N) around every pixel P_0 (Equation 2).[23,24]

$$\mathbb{N}(P_0) = \{P(x,y,n) s.t. \|(x,y) - (x_0,y_0)\| \leq S\ px \ \text{and} \ |n - n_0| \leq N\ \text{frames}\} \quad (2)$$

Given an exposure time T, speckle contrast values then were used to calculate an estimate of blood

velocity that is proportional to a parameter $1/\tau_c$, where $\tau_c(P_0)$ is the correlation time of intensity fluctuations (Equation 3).[25,26] A plot of $1/\tau_c$ is indicative of blood flow velocity (BFV) at a pixel and, when calculated within specific vessels of interest, resulted in an output image with BFV depicted in pseudo-color (Fig. 1C).

$$[K(P_0)]^2 = \frac{\tau_c(P_0)}{T}\left\{2 - \frac{\tau_c(P_0)}{T}\left[1 - \exp\left(-\frac{2T}{\tau_c(P_0)}\right)\right]\right\} \quad (3)$$

To compare differences in image quality produced by a standard fundus camera and the XyCAM HRI prototype, the reference color fundus (CF) images (acquired using the Topcon TRC 50DX) and XyCAM HRI prototype green light (GL) fundus images were statistically compared. The best CF image (i.e., the CF image that was visually the least blurry and had the highest vessel-to-background contrast) was chosen from Trial 3, while two GL images representing both use cases were obtained from the best imaging session in Trials 1 and 2. GL images subsequently were enhanced in MATLAB by: (1) performing median filtering of the image using a 5×5 neighborhood, (2) normalizing intensities within a defined ROI, and (3) applying Contrast-limited Adaptive Histogram Equalization (CLAHE); these enhanced GL images represent the images that would be presented to the XyCAM prototype operator for assessment in a clinical setting. Only the green component of the CF images was isolated and used in subsequent analyses. For each subject, all visible vessels then were manually segmented from the background to form two binary masks, where the masks were selected from areas of each CF and GL image that represented the same ROI around the ONH. The average pixel intensities of the background and vessel masks were calculated and used to determine each image's overall contrast-to-noise ratio (CNR). A paired Student's *t*-test then was used to compare the CNR between stabilized versus handheld use case GL images and between the GL and CF images across subjects ($\alpha = 0.05$).

Intra- and Intersession Reproducibility

Since indices of flow and velocities through vessels are mathematical computations of BFV estimates, reproducibility analysis was performed on these BFV estimates. BFV estimates from four types of ROIs were assessed for reproducibility. The four ROIs were a segment of the second branch of the central retinal artery, a segment of the second branch of the central retinal vein, all manually discriminable vessels with diameters >5 pixel widths, and an annular region surrounding the optic disc. In each of 24 BFV images per imaging session, the mean value of all pixels within each of the aforementioned ROIs was estimated. The coefficient of variation (CV) of these mean BFV values was calculated and reported. Reproducibility analysis was performed for images acquired using stabilized and handheld use cases and compared across subjects using a paired Student's *t*-test ($\alpha = 0.05$). In addition, a more nuanced assessment of blood flow variability in arteries versus veins was explored across sessions, where a paired Student's *t*-test was used to compare mean and CV measures for vessel segments of the second branch of the CRA versus CRV ROIs across subjects.

Comparison of Arterial and Venous Flow Velocities

In addition, the time course of BFV for each vessel ROI was evaluated within an individual session and a correlation analysis was conducted to identify any significant linear correlations in BFV time courses between vessel ROIs ($\alpha = 0.05$). Specifically, this analysis sought to determine if the XyCAM HRI prototype could resolve pulsation patterns that occurred over the course of an image acquisition (<3.0 seconds), and if these patterns were reproduced across same-type vessels (i.e., arteries or veins).

Results

Quality of Images Obtained by XyCAM Prototype

As shown in Figure 2, the XyCAM HRI prototype successfully produced fundus photographs as well as complemented these images with blood flow information. The FOV was approximately 20° and it was possible to image a region around the ONH by instructing the subject to fixate his gaze on an appropriately positioned target. Acquisition of fundus and laser speckle images was achieved under three seconds, with each imaging session requiring two to three minutes for focusing, processing, and saving the image data.

Across subjects, the stabilized use case of the XyCAM HRI prototype produced GL fundus photographs with a vessel-to-background contrast (VBC) profile (estimated in the form of CNR) that was not significantly distinct ($P = 0.08$, Fig. 3) from the VBC in images obtained during the handheld use case and

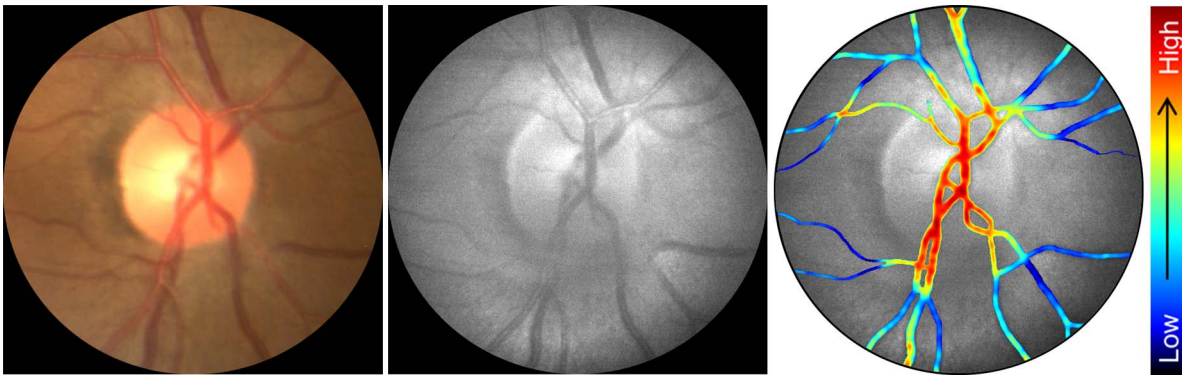

Figure 2. Illustration of the ability of XyCAM HRI prototype to complement traditional fundus photographs with blood flow information. *Left*: Reference color fundus images acquired using a Topcon TRC 50DX fundus photography device. *Middle*: Enhanced green light fundus images acquired using the XyCAM HRI prototype. *Right*: Image depicting blood flow in retinal arteries and veins in pseudocolor.

using a Topcon TRC50. XyCAM GL images acquired during the stabilized use case also revealed a similar VBC (CNR = 0.30 ± 0.14) to the reference color fundus images (CNR = 0.23 ± 0.15, $P = 0.29$). In addition, the VBC of XyCAM images acquired during the handheld use case (CNR = 0.40 ± 0.20) was significantly higher than the reference color fundus images ($P = 0.01$).

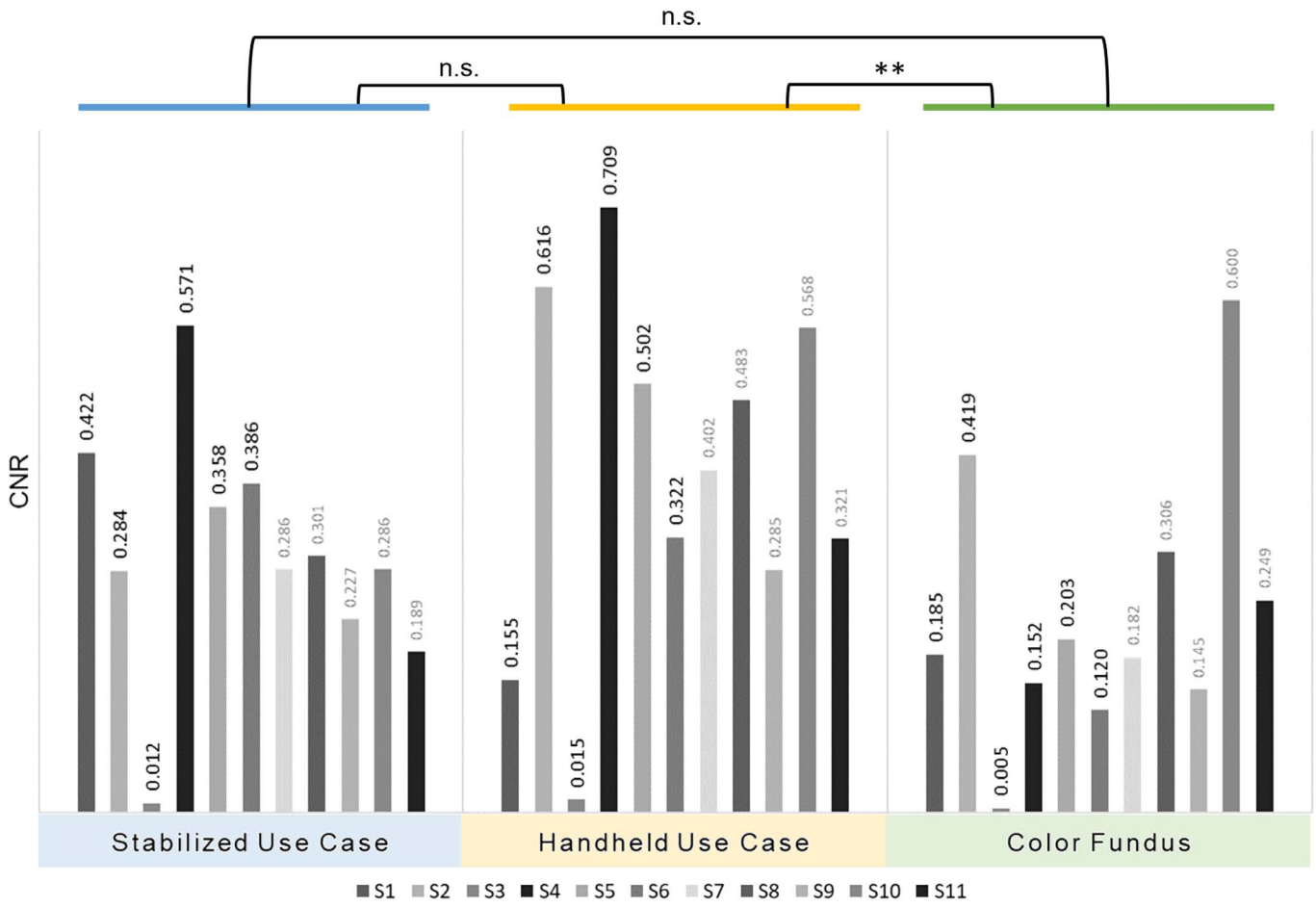

Figure 3. Comparison of each imaging modality's ability to discriminate vessels from background retinal tissue, as measured by CNR. *$P < 0.05$, **$P < 0.01$. n.s, not significant; S1–S11, subject IDs (refer to Table 1).

Table 3. Summary of Intrasession Variation in BFV Estimates in Different Regions of the Vasculature Across Six Assessed Subjects

CV		Stabilized Use Case	Handheld Use Case
Overall retinal perfusion	Mean	9.57%	10.61%
	SD	3.93%	4.35%
Overall vascular component	Mean	8.71%	10.41%
	SD	2.55%	3.50%
Selected arteries	Mean	9.60%	12.15%
	SD	2.41%	3.76%
Selected veins	Mean	7.82%	8.33%
	SD	2.38%	1.44%

Reproducibility of XyCAM HRI Prototype-Based Blood Flow Estimates

Table 3 lists the CV across 24 measurements of specific regions of the retina obtained sequentially as part of the imaging session. The mean CVs encountered during handheld use were consistently higher than those encountered during stabilized use for each type of ROI ($P < 0.02$). However, as shown in Figure 4, when mean BFV estimates over an annular ROI surrounding the optic disc were considered, estimates generated during the stabilized and handheld use cases were significantly similar with a coefficient of determination (R-squared value) of 0.96 ($P < 0.01$).

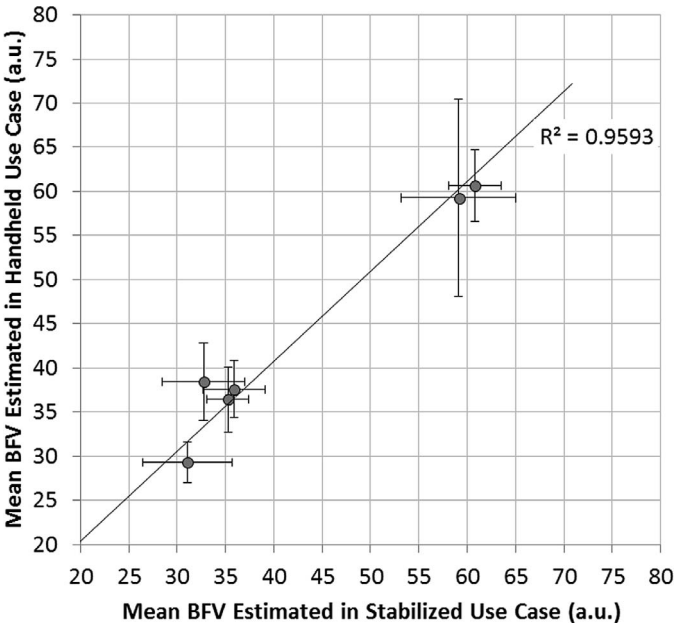

Figure 4. Comparison of mean BFV measurements of the same retinal field of view of the same subject obtained during handheld and stabilized use of the XyCAM prototype.

Assessment of Arterial and Venous Blood Flow Characteristics

Table 3 further highlights the difference in CVs in BFV estimates from arterial and venous regions. While the CVs in arterial regions were significantly greater than the CVs in venous regions in the stabilized use case ($P < 0.05$), the difference in the CVs in the two types of vessels during the handheld use case was only weakly significant ($P < 0.11$). However, as shown in Figure 5, the peak velocity estimates in arteries were significantly higher than those in veins ($P < 0.05$).

Discussion

Preliminary clinical results in 11 healthy individuals validated two important aspects of the XyCAM HRI prototype. First, these results demonstrated the device's ability to acquire fundus photographs with the same or better level of clarity as standard color fundus photographs. Second, these results demonstrated the ability of the XyCAM HRI prototype to reproducibly acquire functional blood flow information from within the human retina. Use of the device in a handheld manner did not significantly affect measurement and reproducibility of image clarity and blood flow measurements, validating its use as a portable retinal blood flow monitor.

While different forms of fundus imaging currently are available in the primary care setting,[27] the combination of retinal blood flow measurement and fundus photography may ultimately improve diagnostic accuracy and facilitate its use in primary care environments for screening and diagnostics. Multiple techniques have been reported that attempt to measure perfusion in the retina, either by providing a binary measurement or by attempting to quantify transit time of a contrast agent. Among them are invasive imaging techniques, such as fluorescein or indocyanine green (ICG) angiography, which require administration of a contrast agent to image retinal vasculature. However, use of the dyes places restrictions on how frequently a technique can be used in acute and longitudinal experiments.[14] Laser Doppler flowmetry has been a popular RBF measurement technique, but is limited by poor reproducibility with coefficient of variation (CV) measured as high as 19.3%.[15] OCTA is a noninvasive technique that uses

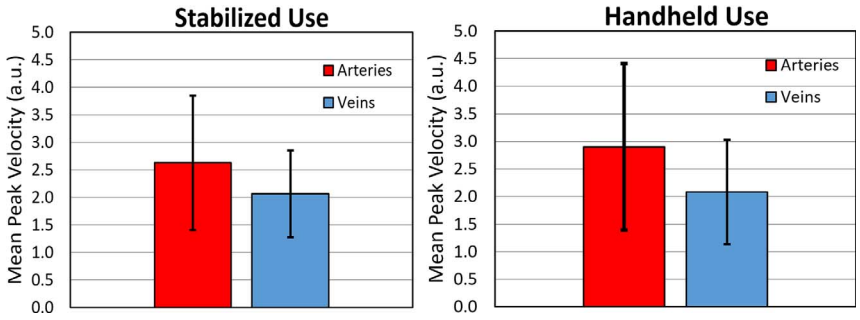

Figure 5. Comparison of estimated peak velocities in arteries and veins across 11 subjects. *$P < 0.04$.

the decorrelation between sequentially obtained OCT data sets as an intrinsic contrast agent to generate images of retinal perfusion. In particular, OCTA has been useful to monitor perfusion status of the microvasculature in the macular region and the optic nerve head.[28,29] While OCTA technology is promising, it currently is neither low-cost nor portable.

Other commercially available laser speckle imaging devices have been used to measure retinal blood flow.[16] Some strengths of the XyCAM HRI include image acquisition at a high frame rate (60 compared to 30 frames per second in other commercially available laser speckle devices[30]), simultaneous acquisition of a red-free retinal image, and spatiotemporal processing for a higher temporal resolution (thus, enabling improved discrimination of dynamic blood flow). To our knowledge, the XyCAM HRI is the first handheld laser speckle imaging device for use in humans. The portability and affordability of this device may allow for greater adoption of this technology within the ophthalmic community as well as at the point of care. For various regions in the retina, we obtained mean CVs that ranged between 7.82% ± 2.38% (for veins) and 9.60% ± 2.41% (for arteries) during the stabilized use case and between 8.33% ± 1.44% (for veins) and 12.15% ± 3.76% (for arteries) during the handheld use cases. This low CV suggests that the XyCAM prototype may offer equivalent or better performance over devices, such as Canon's Doppler Blood Flowmeter (median CV > 19%)[15] and Softcare's LSFG-NAVI system, which was shown to measure blood flow in retinal vessels with a CV of 8.4% ± 5.6% (for veins) and 10.9% ± 9.9% (for arteries).[16] Retinal blood flow is inherently pulsatile and, therefore, manifests itself into time-varying measurements influencing the CV. As expected, the mean CV of BFV values in arterial regions was observed to be significantly higher than in venous regions in the stabilized use case, but not in the handheld use case suggesting that motion during handheld use may have a confounding role.

While this study presents promising human data on a novel technology, we noted that it had a relatively small sample size, but paves the way for an upcoming large-scale clinical trial. We further noted that the best image data from the XyCAM HRI prototype were obtained with a dilated pupil diameter of ≥5 mm, which is a limitation of the technology that may be improved in subsequent updates. We did not assess choroidal blood flow, which may also have a role in ocular and systemic disease.[31]

Given that retinal diseases and systemic conditions affecting retinal vasculature can be diagnosed and/or assessed by analyzing the morphology and physiology of the vascular environment, the XyCAM HRI prototype presents as a suitable low-cost candidate for retinal analytics in a primary care setting that provides as-good-as or better fundus measurements when compared to color fundus photography and has the additional benefit of vascular physiology measures.

Acknowledgments

Supported by the Maryland Technology Enterprise Institute (MTECH) through the Maryland Industrial Partnerships (MIPS) award, in part by a Business Development Award provided to Vasoptic Medical, Inc. by the BioMaryland Center, and by an NIH Career Development Award (K23EY025014; OJS).

Disclosure: **A. Rege**, Vasoptic Medical, Inc. (F, P); **S.I. Cunningham**, Vasoptic Medical, Inc. (F); **Y. Liu**, Vasoptic Medical, Inc. (F, P); **K. Raje**, Vasoptic Medical, Inc. (F, P); **S. Kalarn**, None; **M.J. Brooke**, Vasoptic Medical, Inc. (F, P); **L. Schocket**, None; **S.**

Scott, None; **A. Shafi**, None; **L. Toledo**, None; **O.J. Saeedi**, None

References

1. Nagaoka T, Sato E, Takahashi A, Yokota H, Sogawa K, Yoshida A. Impaired retinal circulation in patients with type 2 diabetes mellitus: retinal laser Doppler velocimetry study. *Invest Ophthalmol Vis Sci*. 2010;51:6729–6734.
2. Cuypers MH, Kasanardjo JS, Polak BC. Retinal blood flow changes in diabetic retinopathy measured with the Heidelberg scanning laser Doppler flowmeter. *Graefe's Arch Clin Exp Ophthalmol*. 2000;238:935–941.
3. Burgansky-Eliash Z, Nelson DA, Bar-Tal OP, Lowenstein A, Grinvald A, Barak A. Reduced retinal blood flow velocity in diabetic retinopathy. *Retina*. 2010;30:765–773.
4. Cheung CY, Ikram MK, Sabanayagam C, Wong TY. Retinal microvasculature as a model to study the manifestations of hypertension. *Hypertension*. 2012;60:1094–1103.
5. Burgansky-Eliash Z, Bartov E, Barak A, Grinvald A, Gaton D. Blood-flow velocity in glaucoma patients measured with the retinal function imager. *Curr Eye Res*. 2015;41:965–970.
6. Kurvinen L, Kyto JP, Summanen P, Vesti E, Harju M. Change in retinal blood flow and retinal arterial diameter after intraocular pressure reduction in glaucomatous eyes. *Acta Ophthalmol*. 2014;92:507–512.
7. McGeechan K, Liew G, Macaskill P, et al. Prediction of incident stroke events based on retinal vessel caliber: a systematic review and individual-participant meta-analysis. *Am J Epidemiol*. 2009;170:1323–1332.
8. Ikram MK, de Jong FJ, Bos MJ, et al. Retinal vessel diameters and risk of stroke: the Rotterdam Study. *Neurology*. 2006;66:1339–1343.
9. Ikram MK, De Jong FJ, Van Dijk EJ, et al. Retinal vessel diameters and cerebral small vessel disease: the Rotterdam Scan Study. *Brain*. 2006; 129:182–188.
10. Ikram MK, Witteman JC, Vingerling JR, Breteler MM, Hofman A, de Jong PT. Retinal vessel diameters and risk of hypertension: the Rotterdam Study. *Hypertension*. 2006;47:189–194.
11. Hurcomb PG, Wolffsohn JS, Napper GA. Ocular signs of systemic hypertension: a review. *Ophthalmic Physiol Opt*. 2001;21:430–440.
12. Wong TY, Klein R, Klein BE, Tielsch JM, Hubbard L, Nieto FJ. Retinal microvascular abnormalities and their relationship with hypertension, cardiovascular disease, and mortality. *Surv Ophthalmol*. 2001;46:59–80.
13. Frost S, Kanagasingam Y, Sohrabi H, et al. Retinal vascular biomarkers for early detection and monitoring of Alzheimer's disease. *Transl Psychiatr*. 2013;3:e233.
14. Bjärnhall G, Mäepea O, Sperber GO, Lindén C, Mönestam E, Alm A. Analysis of mean retinal transit time from fluorescein angiography in human eyes: normal values and reproducibility. *Acta Ophthalmol Scand*. 2002;80:652–655.
15. Guan K, Hudson C, Flanagan JG. Variability and repeatability of retinal blood flow measurements using the Canon laser blood flowmeter. *Microvasc Res*. 2003;65:145–151.
16. Aizawa N, Yokoyama Y, Chiba N, et al. Reproducibility of retinal circulation measurements obtained using laser speckle flowgraphy-NAVI in patients with glaucoma. *Clin. Ophthal*. 2011;5:1171–1176.
17. Jia Y, Bailey ST, Wilson DJ, Tan O, Klein ML, Flaxel CJ. Quantitative optical coherence tomography angiography of choroidal neovascularization in age-related macular degeneration. *Ophthalmology*. 2014;121:1435–1444.
18. Hayashi H, Okamoto M, Kawanishi H, et al. Ocular blood flow measured using laser speckle flowgraphy during aortic arch surgery with antegrade selective cerebral perfusion. *J Cardiothorac Vasc Anesth*. 2016;30:613–618.
19. International-Organization-for-Standardization. ISO 15004-2:2007 Ophthalmic instruments – Fundamental requirements and test methods – Part 2: Light hazard protection. 2007. Available at: https://www.iso.org/standard/38952.html.
20. International-Electrotechnical-Commission. IEC 60825-1-2001 Safety of Laser Products—Part 1: Equipment Classification, Requirements, and User's Guide. 2001. Available at: https://shop.textalk.se/shop/ws26/40626/files/full_size_-_for_start_page_banner/iec60825-1%7Bed1.2%7Den.pdf.
21. Fercher AR, Briers JD. Flow visualization by means of single-exposure speckle photography. *Opt Commun*. 1981;37:326–330.
22. Cheng H, Luo Q, Zeng S, Chen S, Cen J, Gong H. Modified laser speckle imaging method with improved spatial resolution. *J Biomed Opt*. 2003; 8:559–564.
23. Duncan DD, Kirkpatrick SJ. Spatio-temporal algorithms for processing laser speckle imaging

data. In: *Proc SPIE 6858: Optics in Tissue Engineering and Regenerative Medicine II*; 2008: 685802–685802.
24. Rege A, Senarathna J, Li N, Thakor NV. Anisotropic processing of laser speckle images improves spatiotemporal resolution. *IEEE Trans Biomed Eng*. 2012;59:1272–1280.
25. Parthasarathy AB, Tom WJ, Gopal A, Zhang X, Dunn AK. Robust flow measurement with multi-exposure speckle imaging. *Opt Exp*. 2008;16: 1975–1989.
26. Ramirez-San-Juan JC, Ramos-García R, Guizar-Iturbide I, Martínez-Niconoff G, Choi B. Impact of velocity distribution assumption on simplified laser speckle imaging equation. *Opt Exp*. 2008;16: 3197–3203.
27. Shi L, Wu H, Dong J, Jiang K, Lu X, Shi J. Telemedicine for detecting diabetic retinopathy: a systematic review and meta-analysis. *Br J Ophthalmol*. 2015;99:823–831.
28. Salz DA, de Carlo TE, Adhi M, et al. Select features of diabetic retinopathy on swept-source optical coherence tomographic angiography compared with fluorescein angiography and normal eyes. *JAMA Ophthalmol*. 2016;134:644–650.
29. Chen CL, Bojikian KD, Xin C, et al. Repeatability and reproducibility of optic nerve head perfusion measurements using optical coherence tomography angiography. *J Biomed Opt*. 2016;21: 65002.
30. Luft N, Wozniak PA, Aschinger GC, et al. Ocular blood flow measurements in healthy white subjects using laser speckle flowgraphy. *PLoS One*. 2016;11:e0168190.
31. Tan KA, Gupta P, Agarwal A, et al. State of science: choroidal thickness and systemic health. *Surv Ophthalmol*. 2016;61:566–581.